Testing the Optolong L-Quad Enhance Filter

by Jim Thompson, P.Eng
Test Report – November 4th, 2023

Introduction:

To the benefit of amateur astronomers, the race to find the best filter design is still going strong. Original equipment manufacturers (OEMs) are releasing new filter designs at a steady pace, to the extent that it seems like there is a new filter on the market every couple of months. One of the most recent examples of this is the new filter just released by the Chinese company Optolong, the L-Quad Enhance filter or L-QEF. The filter is a new offering in the multi-broadband filter category and is the focus of this test report.

Objective:

The objective of this test report is to evaluate the performance of the new Optolong L-QEF, comparing it to other existing filters of the same type. The list of filters considered in this test report is provided below and is illustrated in Figure 1 (quoted price for 2" version):

- Astronomik UV/IR Block – $99.95USD (for reference)
- IDAS LPS-D2 – $189USD (discontinued)
- IDAS LPS-P3 – $189USD (replaced by LPS-D3, and more recently NGS-1)
- Antlia Triband RGB Ultra – $179USD
- Optolong L-Pro – $199USD
- Optolong L-QEF – $199USD

Figure 1   Photo of Filters Under Test

Note that, by my own definition, the Antlia filter is technically not a multi-broadband filter. It's ~30nm wide pass bands put it, just barely, into the bottom of the multi-narrowband category. My samples of the L-QEF, L-Pro, and LPS-P3 filters were provided courtesy of their respective OEMs. The other filters considered in the testing were purchased. Filter performance was evaluated based on the increase in contrast between the observed object and the background,

which is a measurable quantity. It was evaluated quantitatively using the measured filter spectra combined with the spectra of several common deepsky objects, and by direct measurement from images captured using each filter and a one-shot colour (OSC) camera. The spectrometer and image data was also used to evaluate the signal-to-noise ratio (SNR) achieved using each filter.

Method:
Testing consisted of data collection from the following sources:

- Spectral transmissivity data, from near-UV to near-IR, measured using an Ocean Optics USB4000 spectrometer; and
- Image data, collected using the following setup:
  - Askar FMA230 apochromatic refractor (f/4.6) with ZWO ASI533MC Pro camera.

The spectrometer data was collected in my basement workshop with the USB4000 and a broad-spectrum light source. Filter spectra were measured for a range of filter angles relative to the light path, from 0° (perpendicular) to 20° off-axis. The spectrometer was recently upgraded, replacing the entrance slit and diffraction grating, to give a wavelength resolution of 0.5nm.

For the purposes of predicting the relative performance of each filter using their measured spectra, a reference spectrum was established for the typical observing objects: bright O-III rich emission nebulae, faint H-α rich emission nebulae, galaxies, reflection nebulae, and comets. The normalized emission spectra used in the analysis are plotted in Figure 2. Reference data used to produce these spectra was found in publicly available resources online, the source object in each case being as follows:

- O-III rich nebulae: M27
- H-α rich nebulae: NGC7000/M42/M8
- galaxies: M51
- reflection nebulae: M45
- comet: combination of 8 different comets from various sources

The image data was collected from my backyard in central Ottawa, Canada where the naked eye limiting magnitude (NELM) due to light pollution is +2.9 on average (Bortle 9+). I switched filter configurations using a ZWO 2" filter drawer. Each time I changed filters I refocused on a conveniently located bright star using a Bahtinov mask. Images were collected on the evening of September 3rd and were of two different targets: the Veil Nebula (NGC6960/6995), and the Andromeda Galaxy (M31). A Moon three days past full was in the sky during my imaging session.
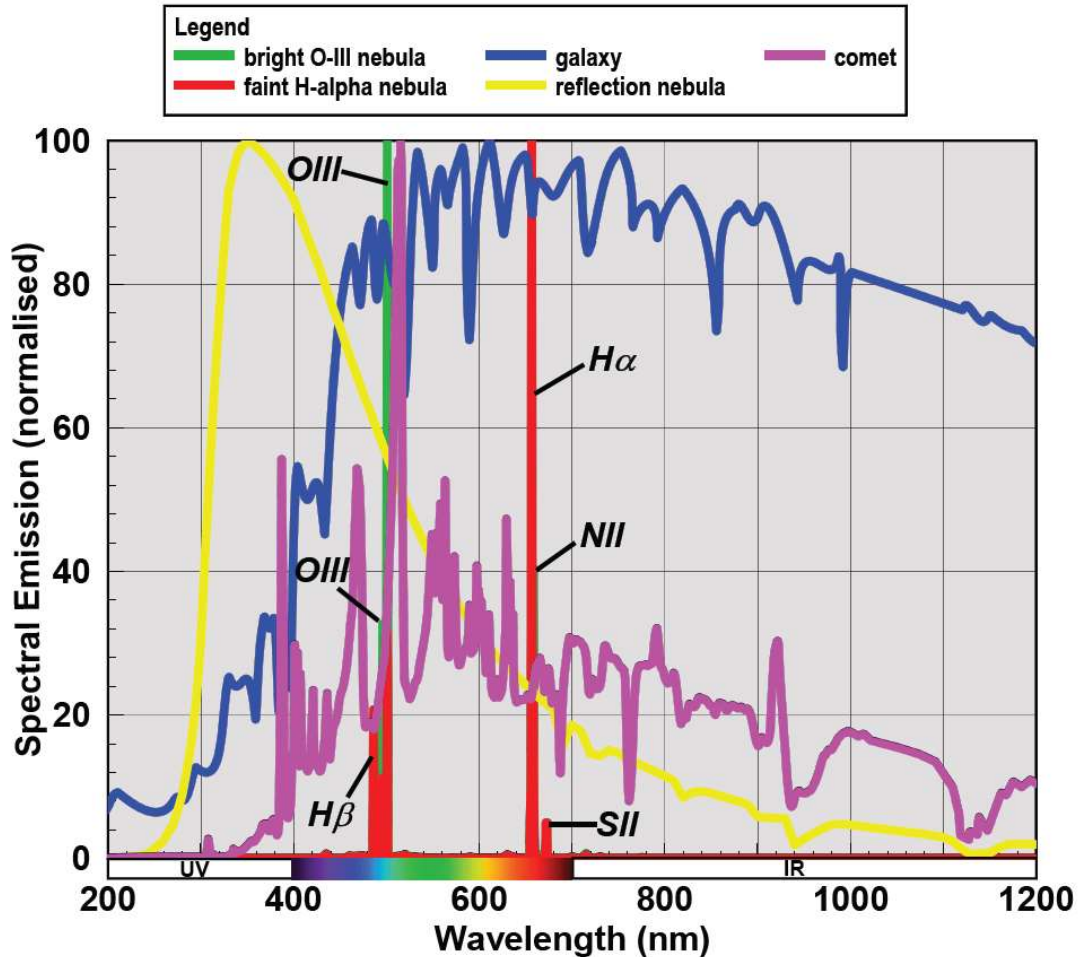
Figure 2   Normalized Emission Spectra for Typical Observing Targets

Results –Spectrum Measurements:

Using the test method mentioned above the spectral transmissivity for each filter was measured for a range of filter angles relative to the light path.   Figures 3 to 8 present a plot of each filter's resulting spectral transmissivity data for the case of the filter perpendicular to the light path. All the filters tested were shown to have high transmission values (>90%) at the important wavelengths for nebula emissions. All of the filters also have a pass band at the blue end of the spectrum, but of varying bandwidth depending on the particular filter. None of the filters pass infrared light, with the exception of the L-Pro which was measured to have a very low transmission of IR between 800 and 950nm.

All the filters tested have wide pass bands as can be seen in Figures 3 to 8. As a result, they all have very low sensitivity to the angle of the light passing through the filter. One can expect consistent performance from any of the filters tested down to f-ratios at least as fast as f/2.
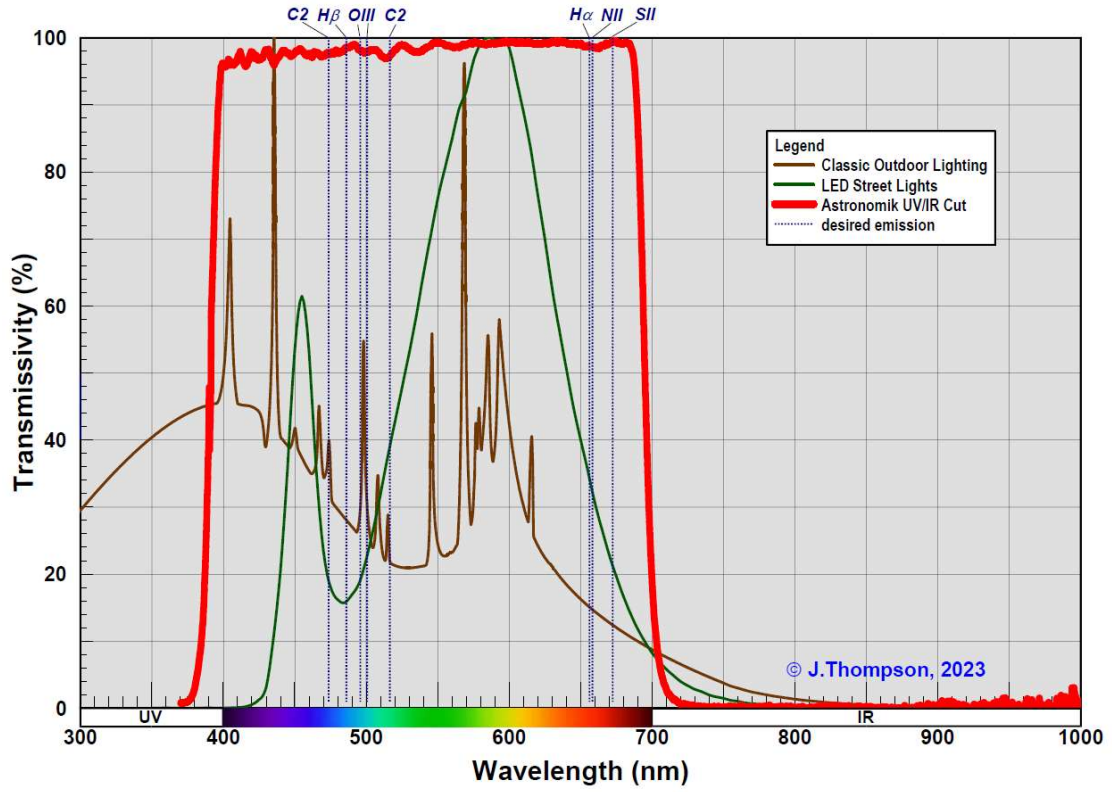
Figure 3   Measured Spectral Response of Tested Filters – Astronomik UV/IR Block
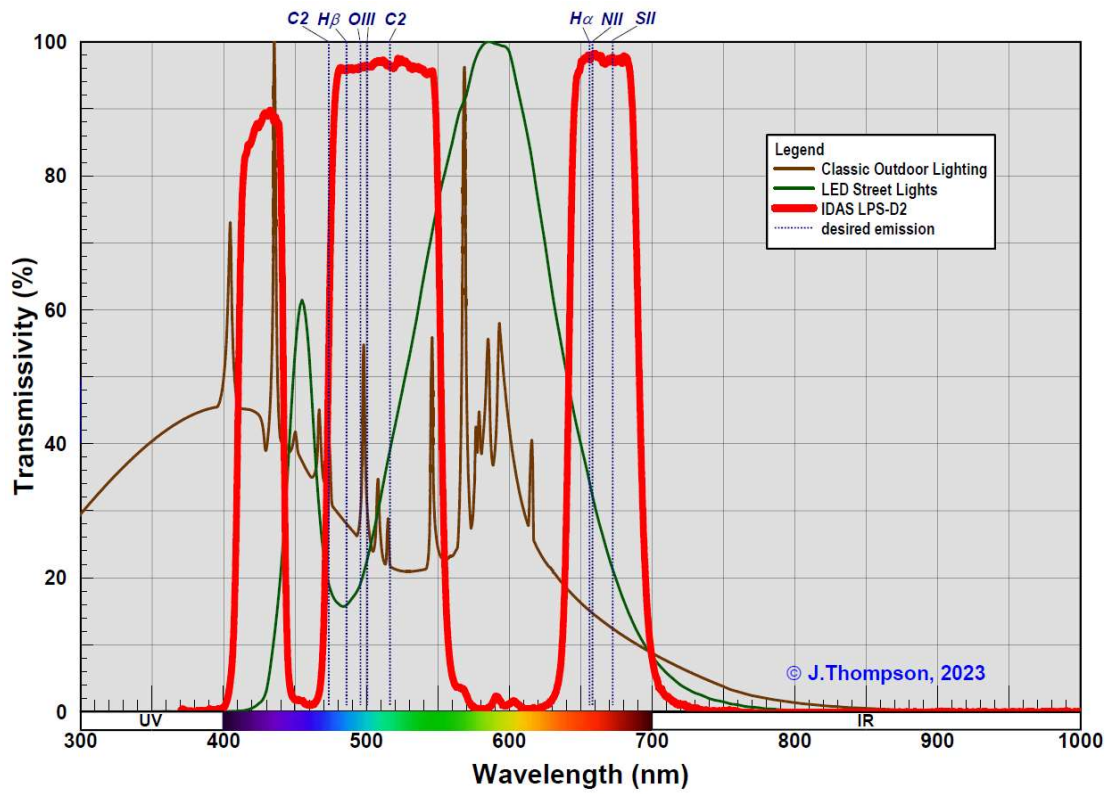

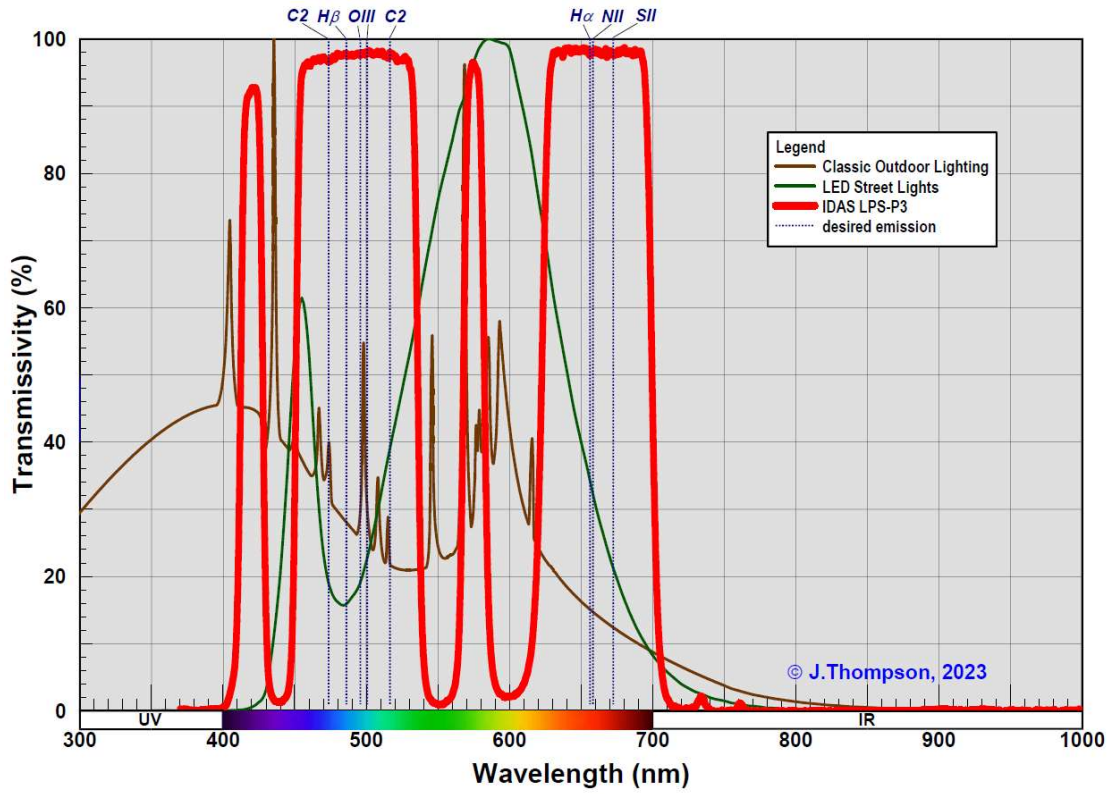**Figure 4   Measured Spectral Response of Tested Filters – IDAS LPS-D2**

Figure 5   Measured Spectral Response of Tested Filters – IDAS LPS-P3
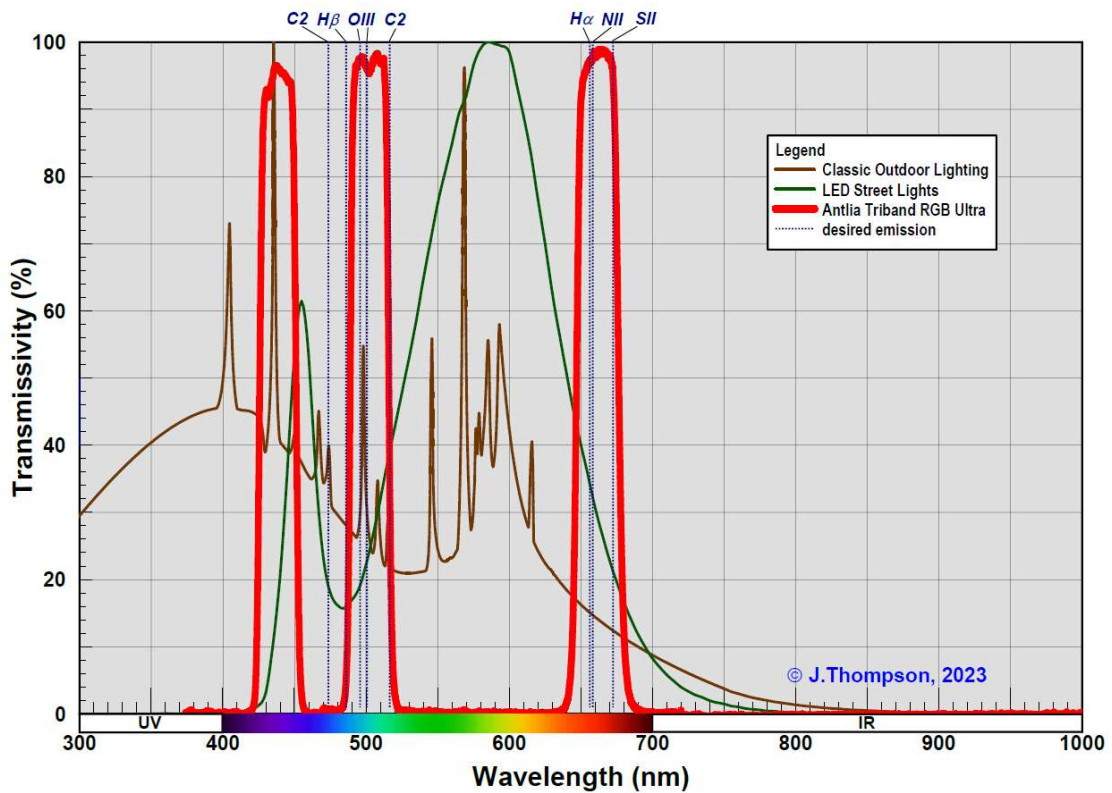

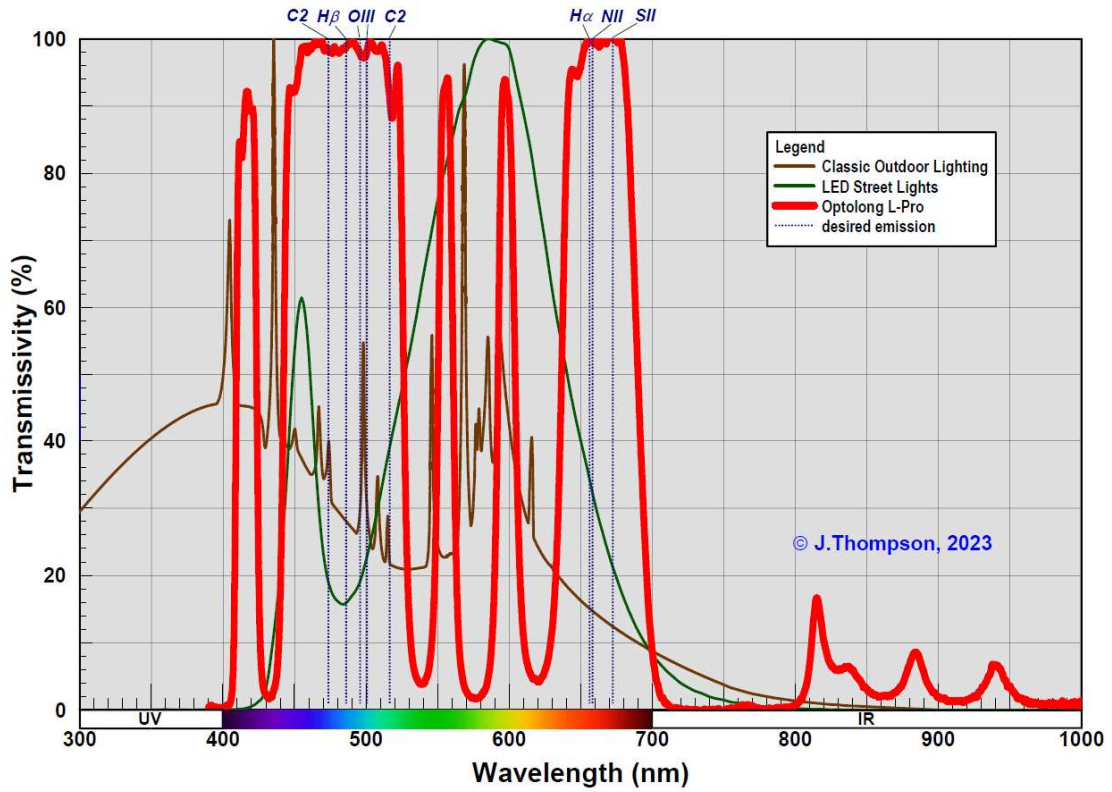**Figure 6   Measured Spectral Response of Tested Filters – Antlia Triband RGB Ultra**

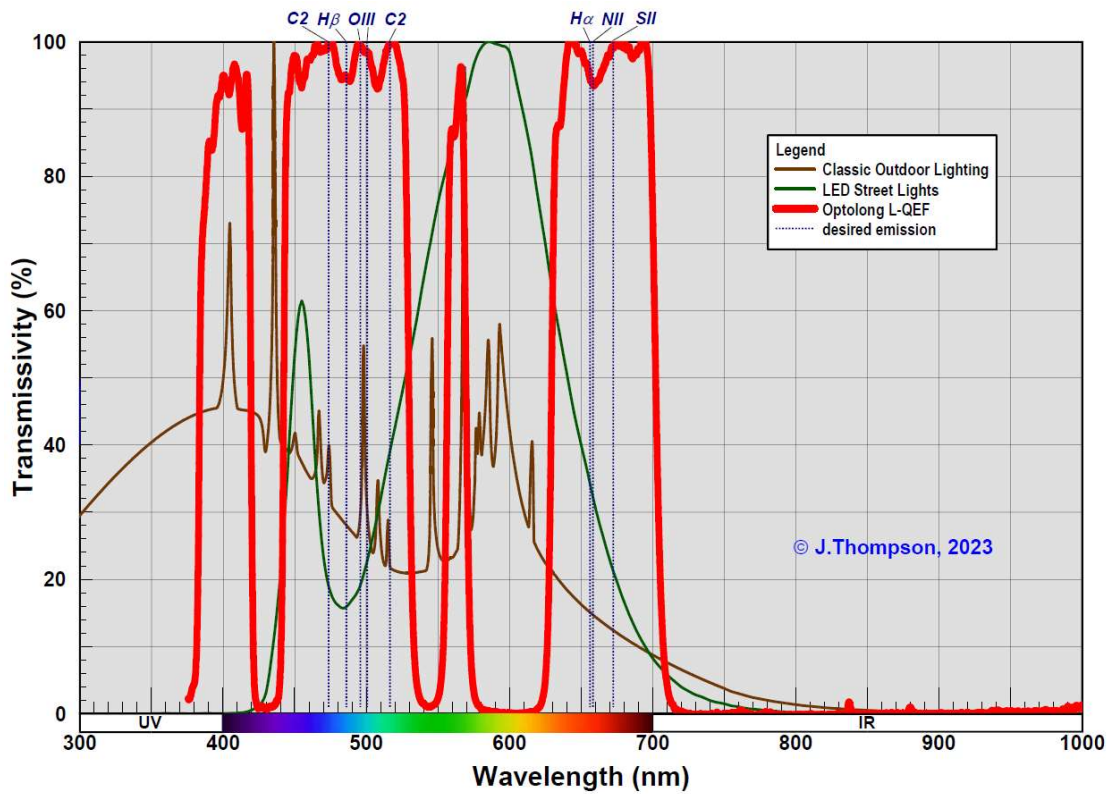**Figure 7   Measured Spectral Response of Tested Filters – Optolong L-Pro**

Figure 8   Measured Spectral Response of Tested Filters – Optolong L-QEF

With the filter spectra in hand, it was possible to extract overall performance related statistics for each filter, such as transmission values at key wavelengths of interest. The filter statistics are provided in Table 1, including a calculated value for percent Luminous Transmissivity (%LT), a single number that describes generally how much light is getting through the filter. The calculated value of %LT depends on the spectral response of the detector, which in this case is assumed to be a modern back illuminated CMOS sensor. The six emission wavelengths of interest for emission nebulae are included in Table 1 (H-β, O-IIIa & b, H-α, N-II, S-II), as well as some key wavelengths associated with comets (CH, Swan C2 bands).

Filter	%LT*	CH (387)	C2 (471.5)	Hbeta (486.1)	O-IIIA (495.9)	O-IIIB (500.7)	C2 (516.5)	C2 (563.5)	Halpha (656.3)	N-II (658.4)	S-II (672.4)
No Filter	100	100	100	100	100	100	100	100	100	100	100
Astronomik UV/IR Block	65.2	19	97	98	98	98	97	99	99	98	99
IDAS LPS-D2	33.3	0	25	96	96	96	96	4	97	98	98
IDAS LPS-P3	41.2	0	98	98	98	98	98	2	99	99	98
Antlia Triband RGB Ultra	17.5	0	1	5	97	96	38	0	97	98	96
Optolong L-Pro	38.9	4	93	96	96	95	93	69	93	92	96
Optolong L-QEF	42.1	75	99	95	99	98	99	90	95	94	99

* calculated assuming spectral QE curve for IMX174M with no UV/IR blocking filter

Table 1   Measured Filter Performance Summary (% Transmission)

Knowing the measured spectral response of the sample filters also allowed me to predict the theoretical relative performance of each filter when imaging different types of object. To do this I used the method I developed back in 2012 which applies the spectral response of the filter and sensor combined with the spectral emission from the object (Figure 1) and background light polluted sky to estimate the apparent luminance observed. To help visualize the results of this analysis I have plotted the predicted % increase in contrast (vs. no filter) for each filter versus the filter's %LT. Figure 9 shows the resulting plot corresponding to filter performance when using a CMOS camera to image a faint H-α rich nebula under a range of sky darkness levels, from a NELM of +2.9 (Bortle 9+) down to +6. Note that these are theoretical predictions of the increase in visible contrast between the object and the background. The absolute values of my predictions may not reflect what a user will experience with their own setup, but the predicted relative performance of one filter to another should be representative. In general, the desired performance for a filter is high contrast increase and high %LT, so the higher and more to the right a filter's performance is in the plot the better. Similar plots of predicted contrast increase for the other object types can be found in Appendix A.

Filters with similar %LT values, i.e. that block LP to a same extent, are predicted to provide roughly the same amount of contrast increase. This includes the LPS-P3, L-Pro, and L-QEF. The LPS-D2 and RGB Ultra are predicted to deliver progressively better contrast as they are blocking progressively more LP. Also calculated using my prediction method is the image SNR, as shown in Figure 10. The predicted SNR values are normalized so that the SNR with no filter equals 1.0, and it is assumed that the same sub-exposure time is used for each filter. Based on my prediction, the image SNR delivered by the different filters trends the same way as the contrast increase, with better SNR from filters that block more LP. A table summarizing all predicted filter performance values is provided in Appendix B.
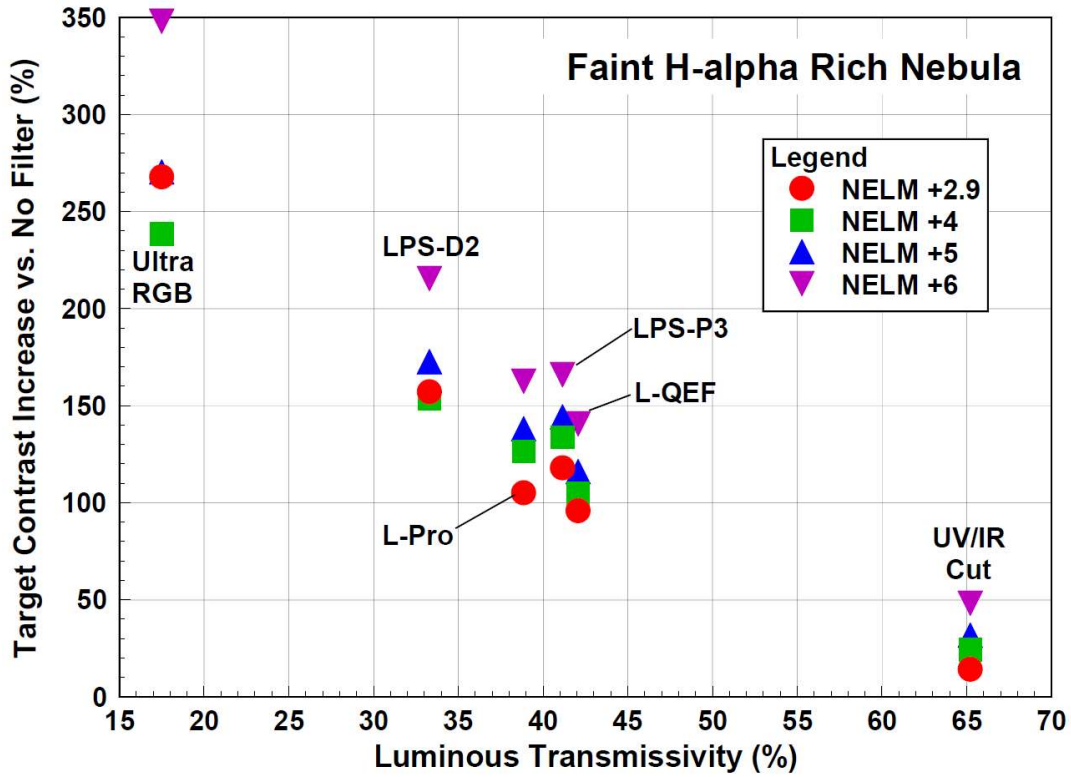
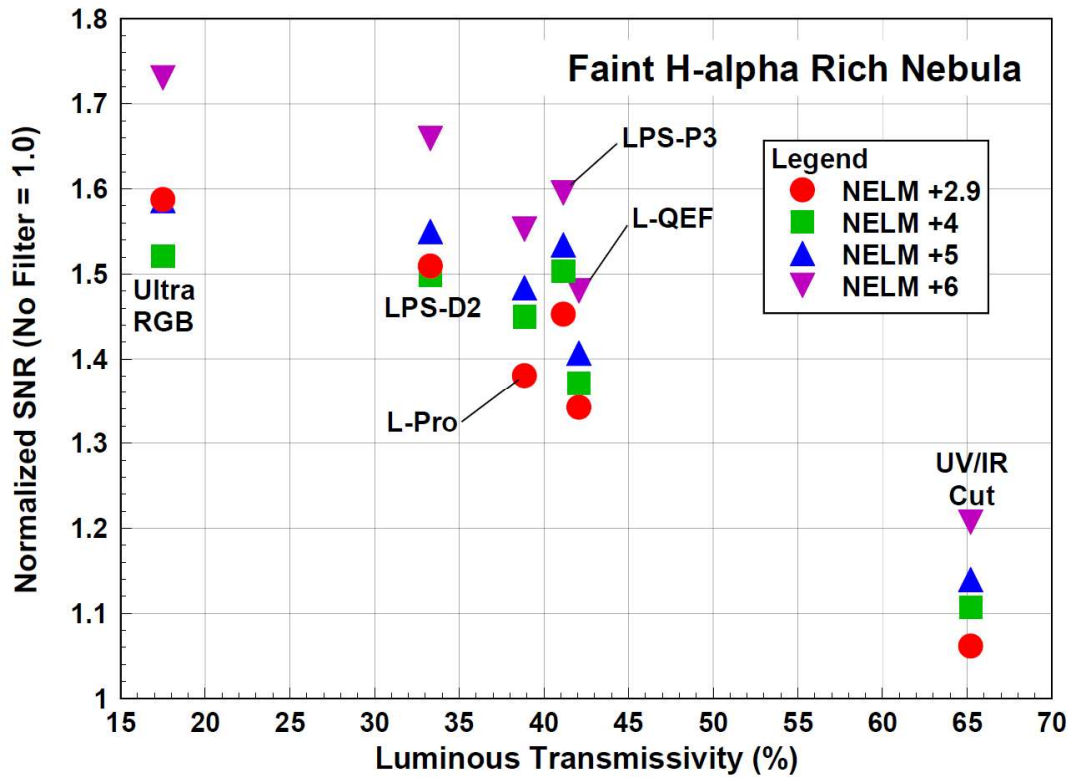**Figure 9   Predicted Filter Performance – Contrast Increase, Faint H-α Rich Nebula**

Figure 10   Predicted Filter Performance - SNR: Back Illuminated OSC CMOS, Bortle 9+ Sky

Results - Imaging:

All image collection on a particular target was done within a one-hour time window. This process was repeated twice, each on a different target as described above. Images were generated by live stacking in Sharpcap, with enough sub's captured in each case to generate a stack with 5 minutes (300s) total exposure. All the images had their histograms adjusted in exactly the same way using Fitswork v4.47, a free FITS editing software, so that they provide as fair a visual comparison as possible. Adjustments were made primarily for white balancing, but a small amount of non-linear stretch was also applied to enhance the visibility of the nebulosity or other faint details in the images.

Images for the first target, the Veil Nebula, are shown in Figure 11. The differences are subtle but it is clear that there is a difference in the extent to which each filter is able to increase the contrast of the nebula. The RGB Ultra filter delivered the best contrast increase, followed by the LPS-D2. The LPS-P3, L-Pro, and L-QEF filters all delivered very similar levels of contrast improvement. These results are consistent with what was predicted from the measured filter spectra.

Images for the second target, the Andromeda Galaxy, are shown in Figure 12. The differences are even more subtle for this target type, with very little perceptible difference between the images in terms of contrast. This observation is also consistent with what was predicted (see contrast increase plots in Appendix A).

Using the raw captured image data I was able to directly measure the contrast increase delivered by each filter, putting a number to what was already observed qualitatively from the images in Figures 11 and 12. This was accomplished by using AstroImageJ to measure the average luminance from two common areas in the images: a dark background area, and a bright deepsky object target area. The particular areas used are illustrated in Figure 13 (red box for target, blue box for background), with these same areas used for all the images from the various filters. Measurements of luminance average and standard deviation were taken from the original unedited FITS files in each colour channel. Contrast increase was calculated from the measured luminance values using the following equations:

Measured Contrast = [measured target luminance – measured background luminance] ÷ measured background luminance

% Contrast Increase = [contrast w/filter – contrast w/out filter] ÷ contrast w/out filter x100
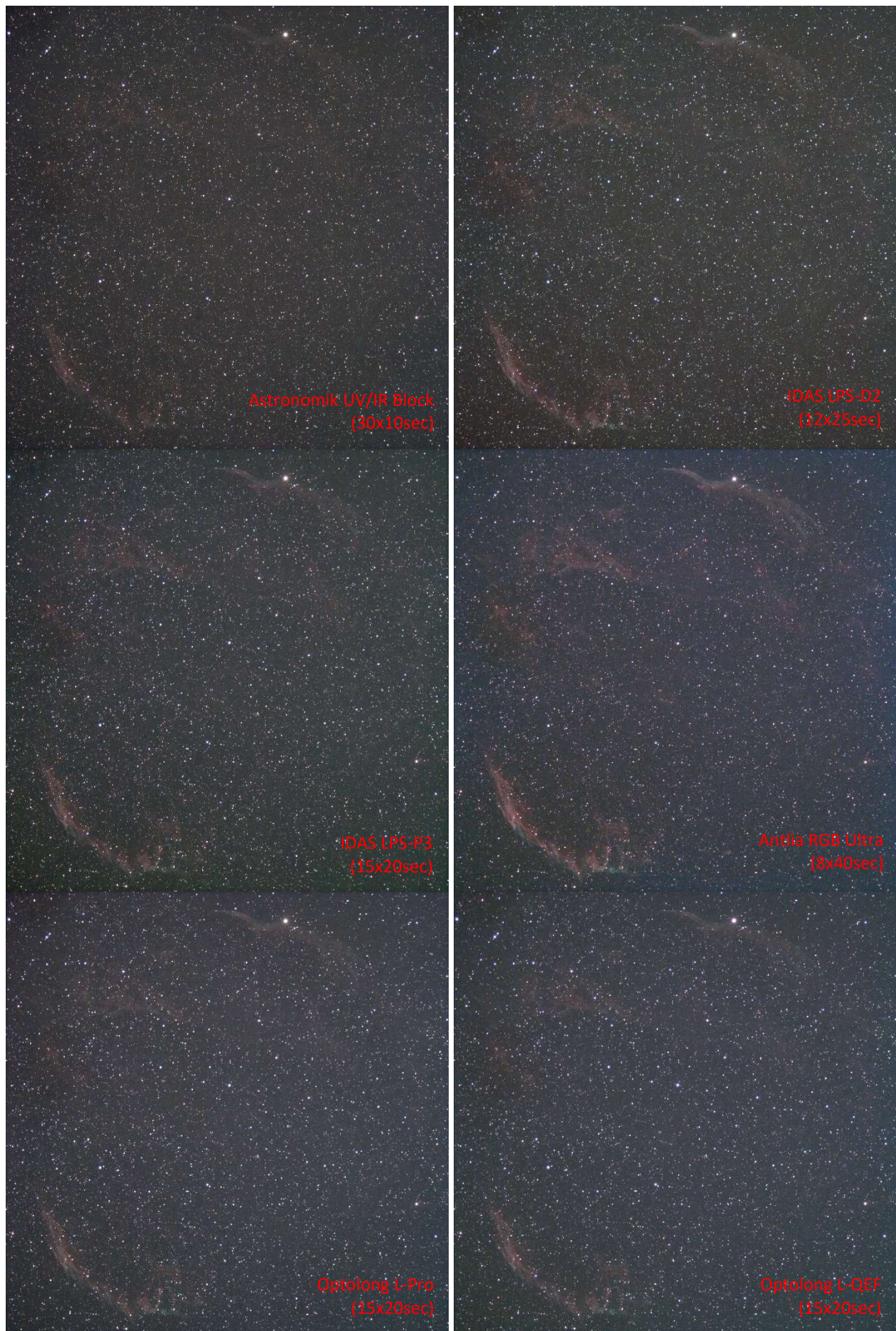
Figure 11   Sep. 3rd Imaging Results – Veil Nebula

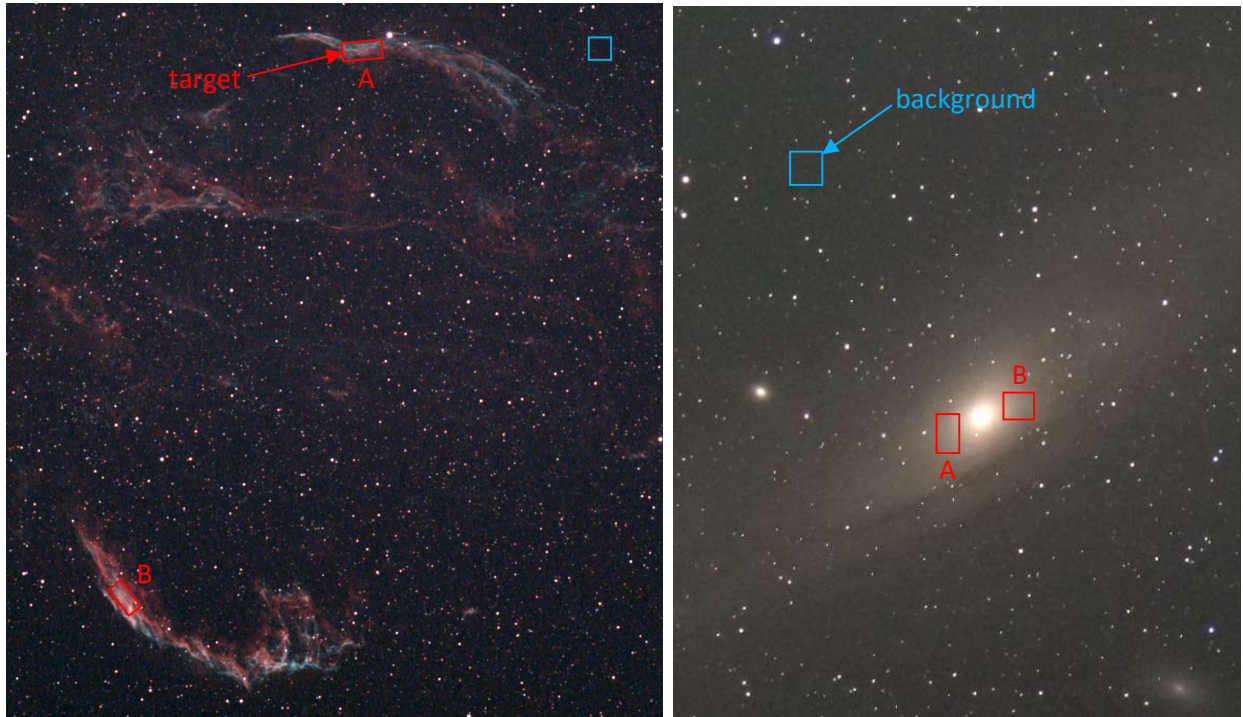**Figure 12   Sep. 3rd Imaging Results – M31 Andromeda Galaxy**

Figure 13   Areas Used for Image Analyses

The resulting contrast increase measurements are plotted in Figure 14, along with the corresponding prediction for each filter. Some offset between measured contrast values and the predictions is expected since the sky conditions during the imaging session (i.e. transparency) is likely not going to be the same as what was assumed in the prediction calculations. That being said, there is a relatively good correlation between the measurements and predictions. The prediction that the new L-QEF delivers effectively the same performance as the L-Pro and LPS-P3 is confirmed by the images. The images also confirm that the extent to which multi-broadband filters increase the contrast of deepsky objects is relatively small when under light polluted skies. It is for this reason that I personally do not refer to multi-broadband filters as "light pollution" filters. In my opinion they are better described as "colour correction" filters. Take for example the appearance of M31 in Figure 12 using the various filters. The image taken using the UV/IR Blocker filter has a yellowish-orange hue that is a result of the light pollution in my backyard. The other filters correct for this un-natural colouration to varying degrees, producing a better colour balanced image but not necessarily one with an improved contrast.

To provide a better impression of the extent to which each tested filter is capable of correcting the colour-cast in an image, consider the versions of my M31 captures in Figure 15. These are the raw stacked images with no post-processing applied, and with their corresponding histogram added to the lower right corner. The camera colour channel gains were not touched between filters from those used for the UV/IR Blocker which has a relatively well colour balanced histogram. All of the other filters tested preferentially attenuated light entering the red colour channel, resulting in a relative boost to blue channel in the images. The green channel is also boosted by these filters, but to varying degrees – this fact being the main differentiator between the filters tested.
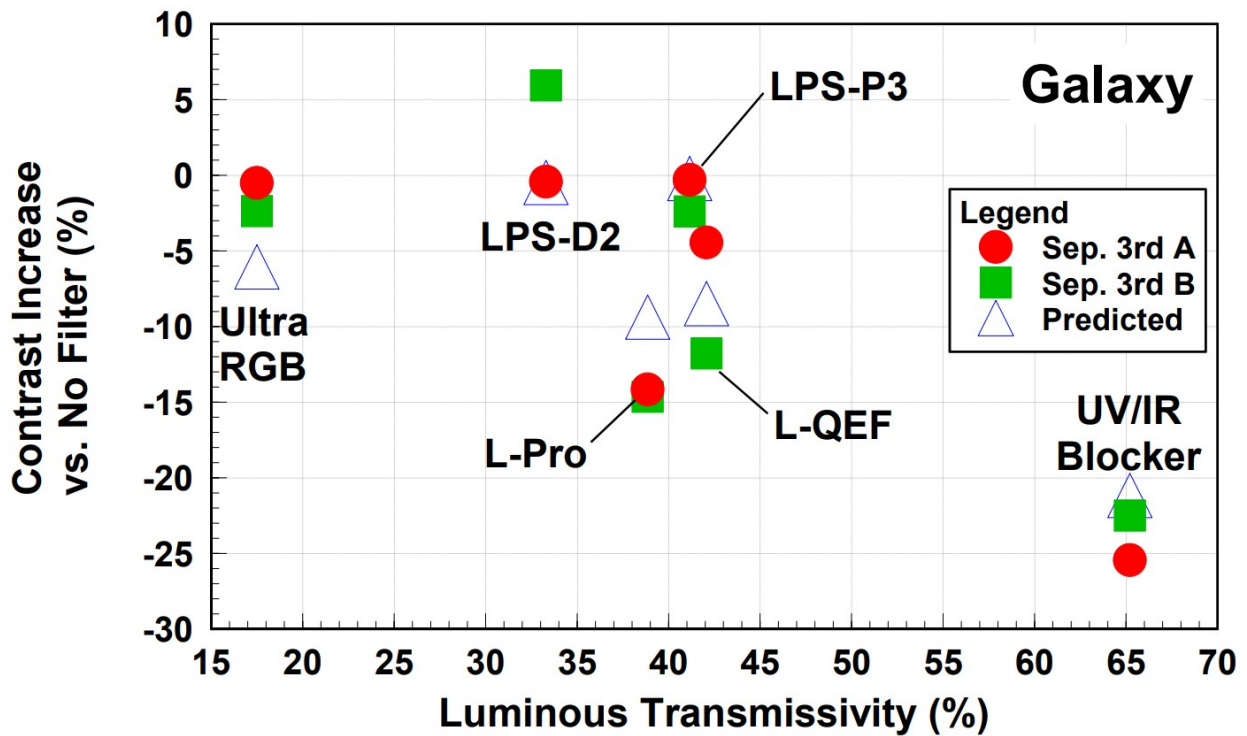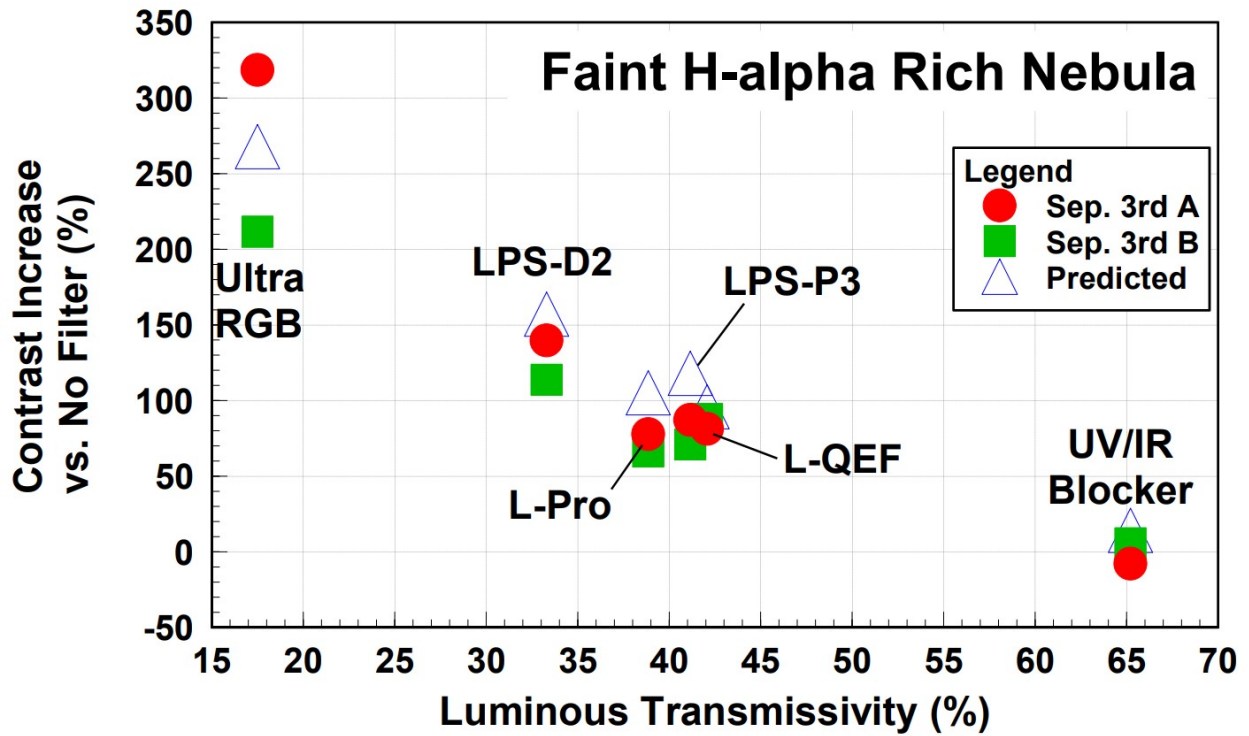
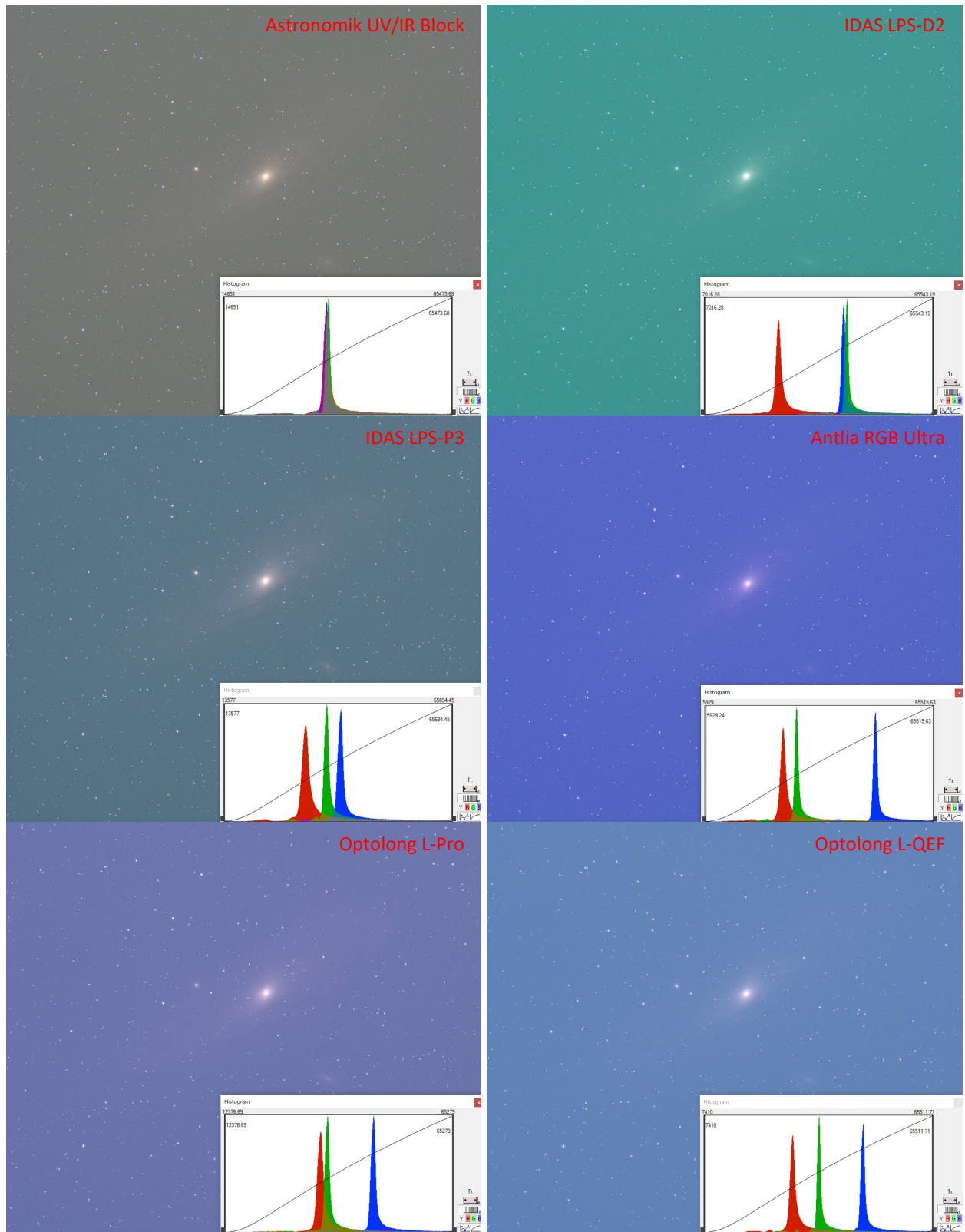**Figure 14   Measured Deepsky Object Contrast Increase vs. Predicted**

Figure 15   Comparison of Raw Stack Colour Balance

As one might expect, having an image's colour channel histograms spread out like shown in Figure 15 has an impact on processing the image data after-the-fact. When the colour channel histogram peaks are closer together, the image is much easier to white balance than when they are far apart.

One final thing to note about multi-broadband filters is the impact they have on the selection of sub-exposure time. I have found that filters that produce a large disparity in the location of each colour channel's histogram peak are difficult to set a proper exposure time for. When the blue channel histogram is located far to the right from the red channel histogram, it is challenging to get enough exposure on the red channel without saturating the blue channel. The RGB Ultra was the worst of the filters tested in this regard.

Multi-Broadband vs. Multi-Narrowband:
I have tested many different types and brands of filters over the years. Based on my experience, all astronomical filters meant to combat light pollution can be sorted into one of four different categories, listed below in order of increasing ability to block LP:

1. Multi-broadband: more than two pass bands, some or all with FWHM >30nm
2. Broadband: one or two pass bands, each with FWHM > 30nm
3. Multi-narrowband: two or more pass bands, all with FWHM < 30nm
4. Narrowband: one pass band, FWHM < 30nm

I further subdivide the broadband category into: Extra Wide, Wide, Medium, and Narrow. Nonetheless, these four basic categories broadly define the capability of the filters fitting these criteria. Multi-broadband filters have the least capability to block LP, while narrowband have the most capability. Depending on what one is trying to achieve, a filter from one category may be more suitable than another. For example: if you are under moderately dark skies and want a well colour balanced image, then a multi-broadband filter may be the right choice.

Most of my observing/imaging is done from a heavily light polluted location. I do however on occasion observe from a moderately dark site, one with a Bortle rating of 5. In July of this year I performed a test from that darker site with the objective of demonstrating how using a filter from the different categories above affected the image collected. The results are summarized in Figure 16. From a darker location the L-Pro filter, an example from the multi-broadband category, delivers a noticeable increase in contrast versus no filter. However, the two images captured using multi-narrowband filters (i.e. NBZ & ALP-T) display much more contrast in the nebulous regions. It is also worth drawing attention to the reflection component of M20 in the upper right. The L-Pro does not diminish the appearance of the blue reflection nebula, but the two multi-narrowband filters do. At the end of the day, the best filter depends on the conditions of your sky AND what it is you are trying to achieve.

No Filter (90x5s)   *Optolong L-Pro (39x10s)*

IDAS NBZ (23x20s)   *Antlia ALP-T (18x30s)*
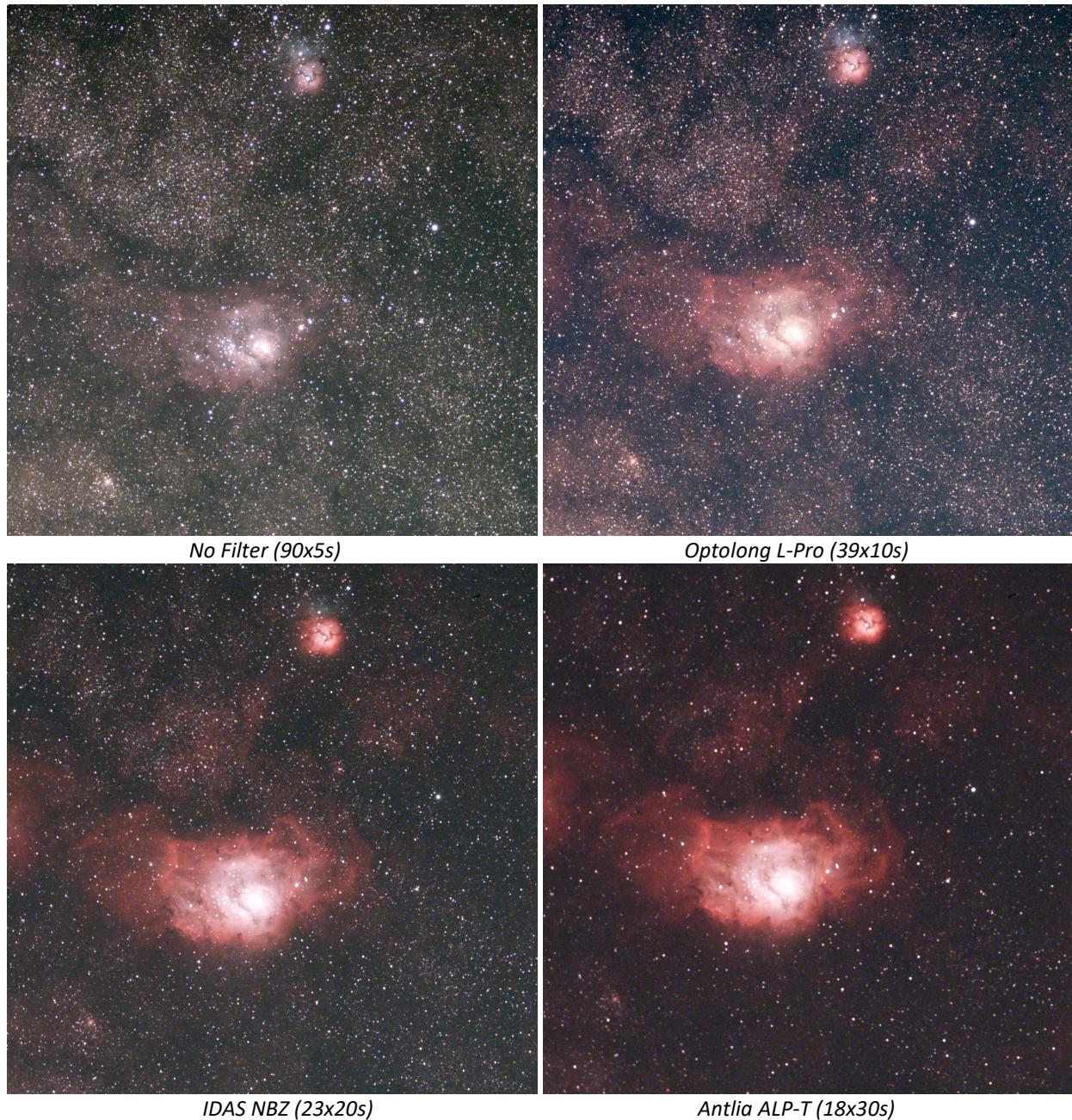
Figure 16   Images from July 18th Filter Test From Bortle 5 Location

Conclusions:

Based on the results of the testing described above, I have made the following conclusions:

1. Based on my test results, the new Optolong L-QEF delivers performance very similar to other existing filters in the multi-broadband category, most notably the Optolong L-Pro and IDAS LPS-P3. Based on the measured filter spectra, the L-QEF may deliver better contrast on reflection nebulae than the existing L-Pro, but I did not have an opportunity to confirm this with imaging.

2. Multi-broadband filters, like the L-QEF, do not block much LP compared to other categories of filter. Their ability to increase the contrast of deepsky objects is poor when under heavily light polluted skies, but is progressively better the darker the sky.
3. Multi-broadband filters are able to help colour correct an image that would otherwise have a colour cast due to light pollution. This capability exists even for heavily light polluted conditions.

If you have any questions, please feel free to contact me.

Cheers!

Jim Thompson
(top-jimmy@rogers.com)

Appendix A – Predicted Increase in Object Contrast vs. No Filter
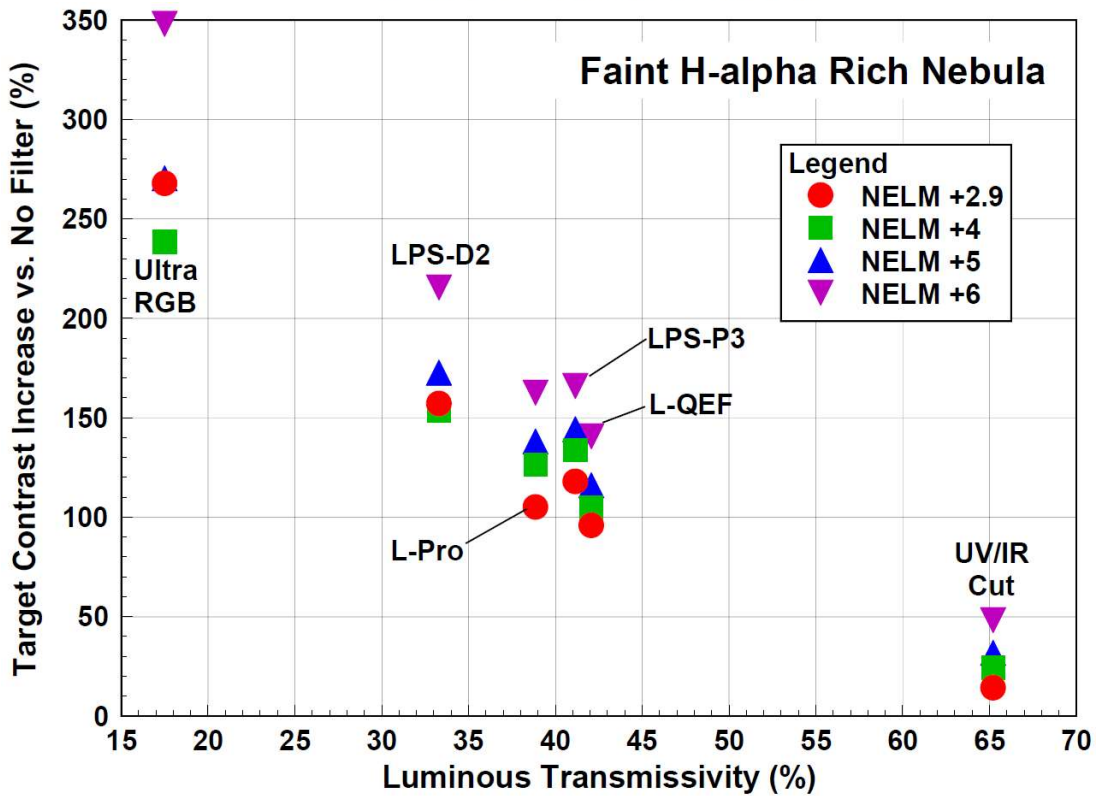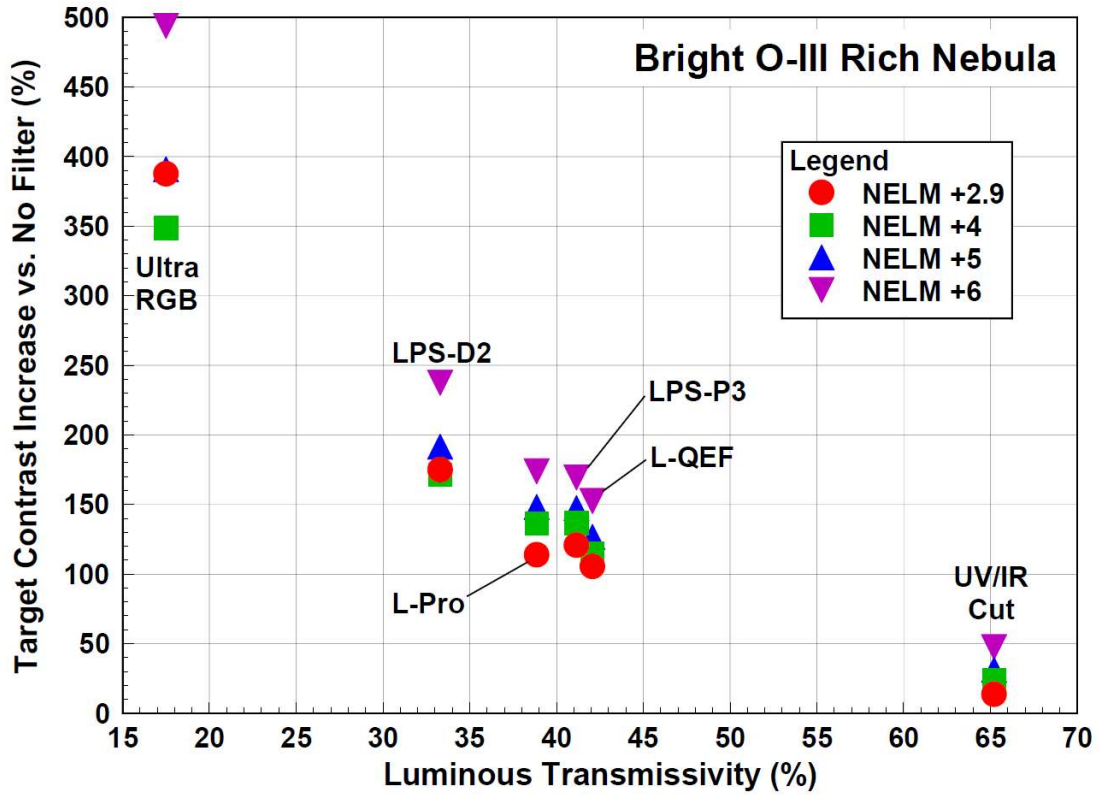
Appendix B – Summary Table of Predicted Filter Performance

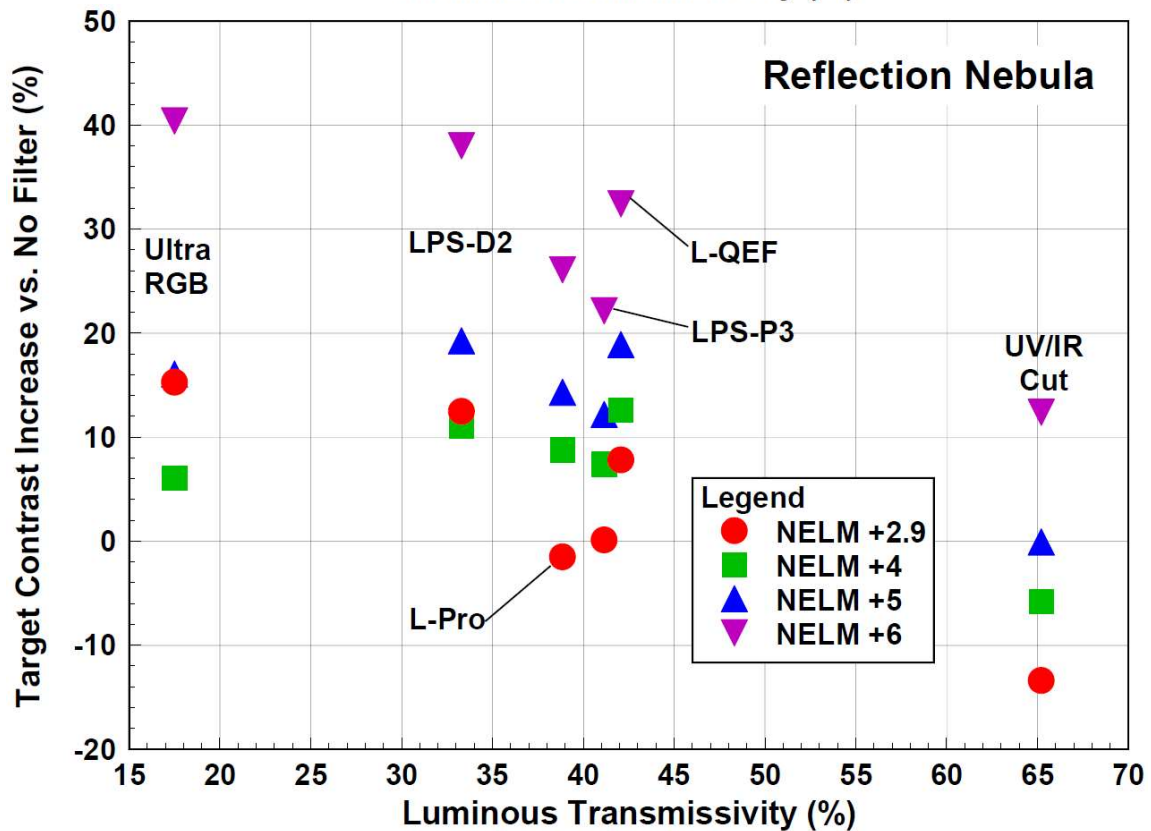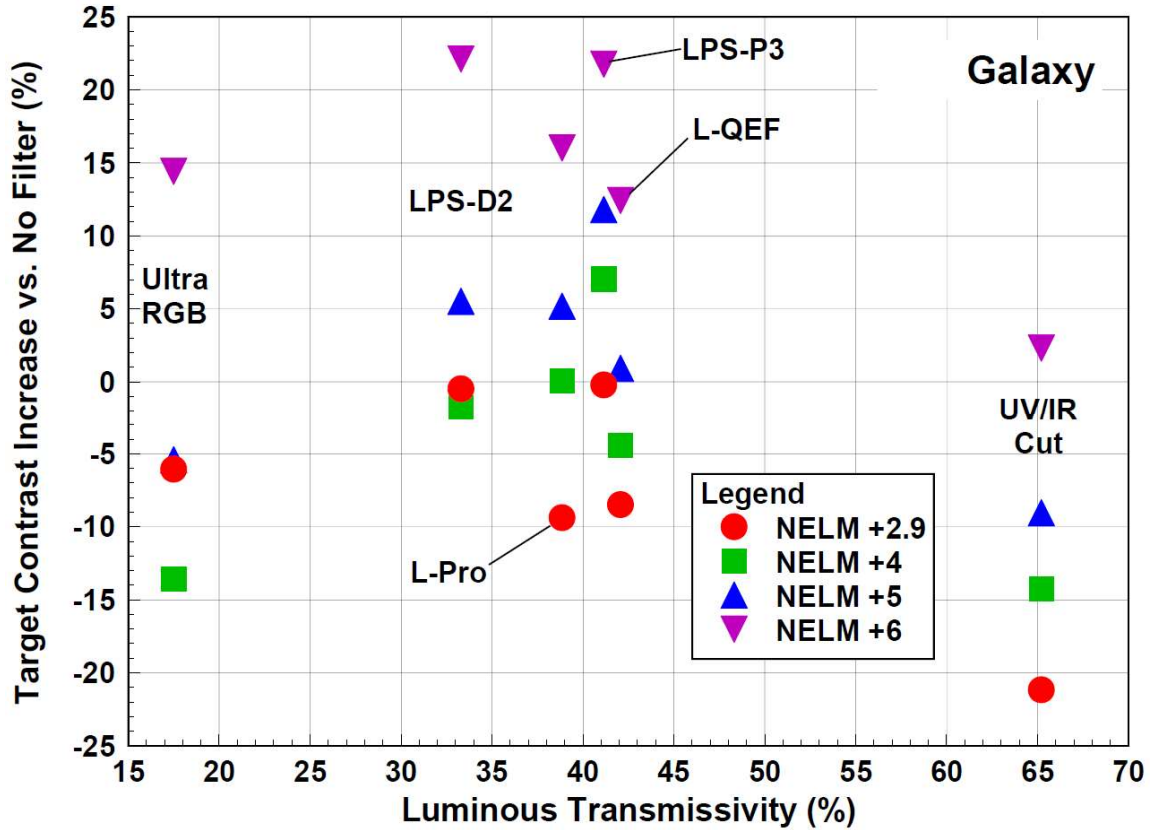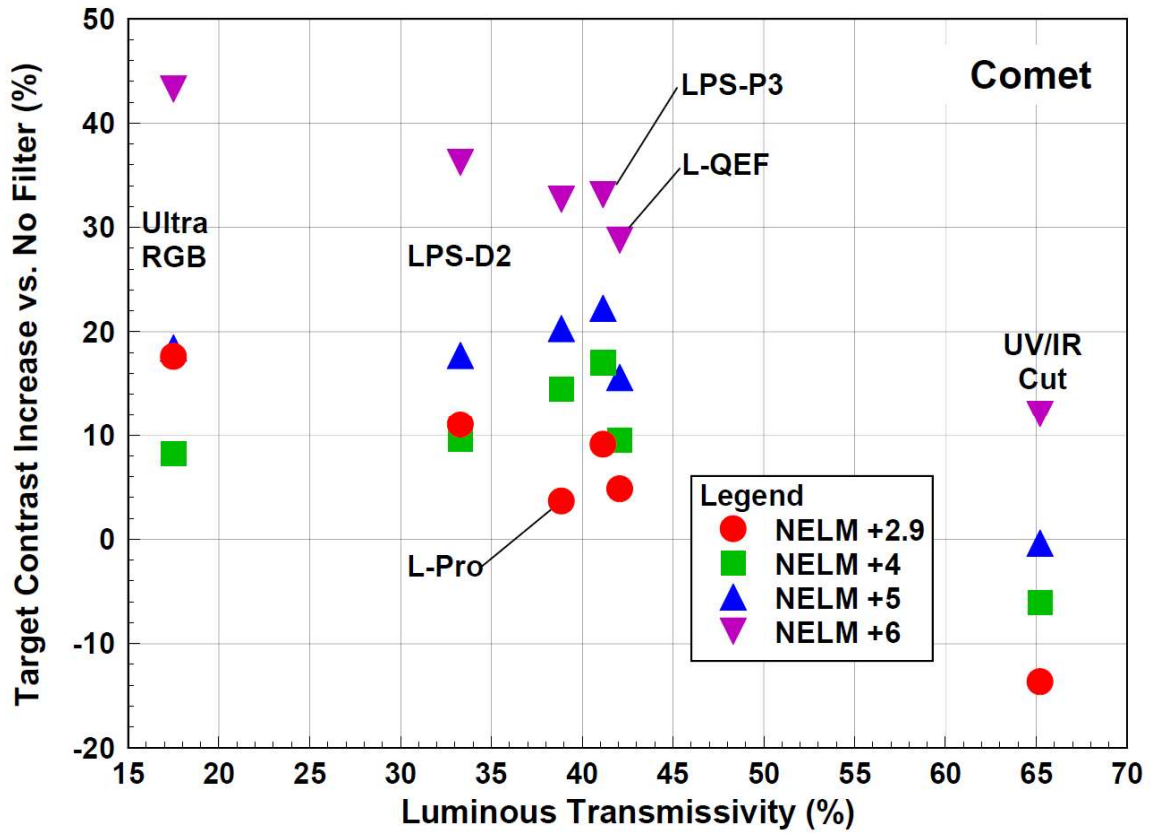| Performance Parameter	Object	NELM	No Filter	Astro. UV/IR Block	LPS-D2	LPS-P3	Ultra RGB	L-Pro	L-QEF
Luminous Transmissivity (%)			100.00	65.21	33.30	41.15	17.50	38.85	42.07
% Contrast Increase vs. No Filter	Bright O-III Nebula	MAG+2.9		13.69	174.97	120.78	387.60	113.89	105.56
		MAG+4		23.69	171.42	136.80	348.53	136.19	114.70
		MAG+5		31.18	191.55	147.37	390.95	148.24	126.69
		MAG+6		47.56	237.41	169.39	493.88	173.84	152.52
	Faint Halpha Nebula	MAG+2.9		14.19	157.12	117.95	267.88	105.10	95.87
		MAG+4		24.23	153.80	133.77	238.40	126.49	104.59
		MAG+5		31.75	172.62	144.20	270.40	138.04	116.01
		MAG+6		48.20	215.51	165.94	348.06	162.59	140.63
	Galaxy	MAG+2.9		-21.17	-0.48	-0.22	-6.06	-9.38	-8.48
		MAG+4		-14.24	-1.77	7.02	-13.58	0.07	-4.41
		MAG+5		-9.04	5.52	11.80	-5.41	5.18	0.92
		MAG+6		2.32	22.11	21.75	14.42	16.03	12.43
	Reflection Nebula	MAG+2.9		-13.40	12.48	0.11	15.28	-1.51	7.81
		MAG+4		-5.79	11.02	7.37	6.04	8.76	12.60
		MAG+5		-0.08	19.26	12.17	16.07	14.31	18.89
		MAG+6		12.39	38.02	22.15	40.41	26.10	32.44
	Comet	MAG+2.9		-13.66	11.03	9.11	17.63	3.66	4.83
		MAG+4		-6.07	9.59	17.03	8.21	14.47	9.50
		MAG+5		-0.38	17.72	22.25	18.44	20.31	15.61
		MAG+6		12.06	36.24	33.14	43.27	32.71	28.78
Fixed Sub-Exposure Time SNR	Bright O-III Nebula	MAG+2.9	1.00	1.06	1.60	1.47	2.08	1.43	1.40
		MAG+4	1.00	1.10	1.58	1.51	1.96	1.50	1.43
		MAG+5	1.00	1.13	1.60	1.51	1.97	1.51	1.44
		MAG+6	1.00	1.18	1.64	1.53	1.98	1.53	1.48
	Faint Halpha Nebula	MAG+2.9	1.00	1.06	1.51	1.45	1.59	1.38	1.34
		MAG+4	1.00	1.11	1.50	1.50	1.52	1.45	1.37
		MAG+5	1.00	1.14	1.55	1.53	1.59	1.48	1.41
		MAG+6	1.00	1.21	1.66	1.60	1.73	1.55	1.48
	Galaxy	MAG+2.9	1.00	0.73	0.58	0.67	0.41	0.61	0.63
		MAG+4	1.00	0.77	0.58	0.69	0.39	0.64	0.64
		MAG+5	1.00	0.79	0.60	0.70	0.41	0.66	0.66
		MAG+6	1.00	0.83	0.64	0.73	0.45	0.69	0.69
	Reflection Nebula	MAG+2.9	1.00	0.81	0.66	0.67	0.50	0.66	0.74
		MAG+4	1.00	0.84	0.66	0.69	0.48	0.70	0.75
		MAG+5	1.00	0.86	0.68	0.71	0.50	0.71	0.77
		MAG+6	1.00	0.92	0.73	0.73	0.55	0.75	0.81
	Comet	MAG+2.9	1.00	0.81	0.65	0.72	0.50	0.70	0.72
		MAG+4	1.00	0.84	0.64	0.73	0.48	0.72	0.72
		MAG+5	1.00	0.86	0.64	0.73	0.49	0.72	0.73
		MAG+6	1.00	0.88	0.65	0.73	0.49	0.72	0.73

Optimized Sub-Exposure Time SNR	Bright O-III Nebula	MAG+2.9	1.00	1.14	2.73	2.20	4.81	2.13	2.05
		MAG+4	1.00	1.23	2.67	2.34	4.35	2.33	2.13
		MAG+5	1.00	1.30	2.81	2.40	4.57	2.41	2.21
		MAG+6	1.00	1.45	3.10	2.53	5.06	2.57	2.39
	Faint Halpha Nebula	MAG+2.9	1.00	1.14	2.57	2.18	3.68	2.05	1.96
		MAG+4	1.00	1.24	2.53	2.34	3.38	2.26	2.04
		MAG+5	1.00	1.32	2.72	2.44	3.69	2.37	2.16
		MAG+6	1.00	1.48	3.13	2.64	4.42	2.61	2.39
	Galaxy	MAG+2.9	1.00	0.79	1.00	1.00	0.94	0.91	0.92
		MAG+4	1.00	0.86	0.98	1.07	0.87	1.00	0.96
		MAG+5	1.00	0.91	1.05	1.12	0.95	1.05	1.01
		MAG+6	1.00	1.02	1.21	1.21	1.14	1.15	1.12
	Reflection Nebula	MAG+2.9	1.00	0.87	1.12	1.00	1.15	0.98	1.08
		MAG+4	1.00	0.94	1.11	1.07	1.06	1.09	1.13
		MAG+5	1.00	1.00	1.19	1.12	1.16	1.14	1.19
		MAG+6	1.00	1.12	1.37	1.22	1.39	1.25	1.32
	Comet	MAG+2.9	1.00	0.87	1.10	1.08	1.16	1.03	1.04
		MAG+4	1.00	0.95	1.08	1.14	1.07	1.12	1.08
		MAG+5	1.00	1.00	1.13	1.16	1.13	1.15	1.11
		MAG+6	1.00	1.08	1.22	1.21	1.26	1.20	1.18